

# Decoding Spatial Complexity in Strongly Correlated Electronic Systems

E. W. Carlson,<sup>1</sup> S. Liu,<sup>1</sup> B. Phillabaum,<sup>1</sup> and K. A. Dahmen<sup>2</sup>

<sup>1</sup>*Department of Physics, Purdue University, West Lafayette, IN 47907, USA*

<sup>2</sup>*Department of Physics, University of Illinois, Urbana-Champaign, IL, 50000, USA*

(Dated: July 21, 2021)

Inside the metals, semiconductors, and magnets of our everyday experience, electrons are uniformly distributed throughout the material. By contrast, electrons often form clumpy patterns inside of strongly correlated electronic systems (SCES) such as colossal magnetoresistance materials and high temperature superconductors. In copper-oxide based high temperature superconductors, scanning tunneling microscopy (STM) has detected an electron nematic on the surface of the material, in which the electrons form nanoscale structures which break the rotational symmetry of the host crystal. These structures may hold the key to unlocking the mystery of high temperature superconductivity in these materials, but only if the nematic also exists throughout the entire bulk of the material. Using newly developed methods for decoding these surface structures, we find that the nematic indeed persists throughout the bulk of the material. We furthermore find that the intricate pattern formation is set by a delicate balance among disorder, interactions, and material anisotropy, leading to a fractal nature of the cluster pattern. The methods we have developed can be extended to many other surface probes and materials, enabling surface probes to determine whether surface structures are confined only to the surface, or whether they extend throughout the material.

There is growing experimental evidence that many strongly correlated electronic systems such as nickelates, cuprates, and manganites exhibit some degree of local inhomogeneity,[1–7] *i.e.*, nanoscale variations in the local electronic properties. Describing the electronic behavior of these materials involves several degrees of freedom, including orbital, spin, charge, and lattice degrees of freedom. Disorder only compounds the problem. Not only can disorder destroy phase transitions, leaving mere crossovers in the wake, it can fundamentally alter ground states, sometimes forbidding long range order. Especially in systems where different physical tendencies compete, disorder can act as nucleation points for competing ground states.

One approach to disentangling disorder from the fundamental correlations induced by strong electron interactions is to put resources toward developing cleaner samples. While this approach is laudable and has led to many key insights and advances in strongly correlated electronic systems, it is also labor intensive and expensive. Even the cleanest sample, when stored over time at finite temperature, will acquire a thermodynamically required concentration of defects. Moreover, in some sense, disorder is intrinsic to the correlated phases, since in most systems the phases of interest happen upon chemical doping, which necessarily introduces disorder. Especially in cuprates, this drive toward cleaner samples or even toward controlling disorder in order to understand the intrinsic electronic states may not be necessary, since even “dirty” samples that have not undergone strict preparation protocols still exhibit the salient feature of superconductivity.[8] Indeed, in any high temperature superconductor, because the pairing scale must also be high, an understanding of the short-distance physics (*i.e.* within a few coherence lengths of the superconduc-

tivity) should be sufficient to understand the origin of pairing.[9] In this sense, long range order of a proposed pseudogap phase is neither necessary to produce superconductivity nor is it necessary in order to understand the superconductivity.

Ultimately, the interplay between many degrees of freedom, strong correlations, and disorder can lead to a hierarchy of length scales over which the resulting physics must be described.[1] While such electronic systems are highly susceptible to pattern formation at the nanoscale, unfortunately most of our theoretical and experimental tools are designed for understanding and detecting homogeneous phases of matter. Therefore, there is a critical need to design and develop new ways of understanding, detecting, and characterizing electronic pattern formation in strongly correlated electronic systems at the nanoscale, especially in the presence of severe disorder effects. Such theoretical guidance will enable more direct contact between theory and experiment in a number of materials, and provide a path forward for understanding “disputed” regions of phase diagrams of strongly correlated materials.

In this paper, we focus on detecting electron nematics and other electronic phases which break the rotational symmetry of the host crystal. Such phases have been proposed and/or observed in a variety of materials and contexts, including  $\text{Sr}_3\text{Ru}_2\text{O}_7$ [12],  $\text{GaAs}/\text{Al}_x\text{Ga}_{1-x}\text{As}$  heterostructures in field[13, 14], and a subset of cuprate superconductors[11, 15–20] such as  $\text{YBa}_2\text{Cu}_3\text{O}_{6+x}$ [16–18], and  $\text{Bi}_2\text{Sr}_2\text{CaCu}_2\text{O}_{8+x}$ [11, 19, 20], as well as the iron arsenic based superconductor  $\text{Ca}(\text{Fe}_{1-x}\text{Co}_x)_2\text{As}_2$ [21]. The state has been proposed to exist in many more systems, such as AlAs heterostructures, the Si(111) surface, elemental bismuth, and both single layer and bilayer graphene.[15, 22–24]

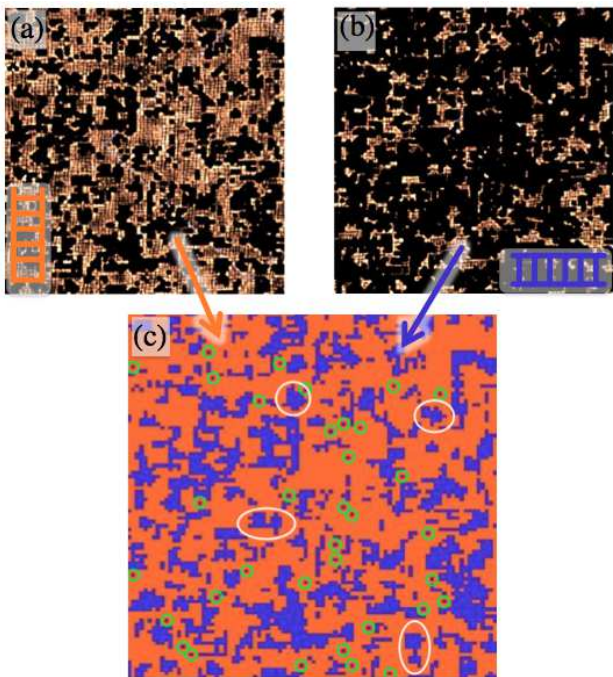


FIG. 1. Mapping of STM data to Ising nematic variables. (a) Masked image[10, 11] of R-map of Dy-Bi2212 showing the regions of the R-map with vertically aligned nematic domains. (b) The complement to panel (a), showing horizontally aligned nematic domains. (c) Mapping to the corresponding Ising geometric clusters, showing several small clusters (circled in green); a smaller number of medium-sized clusters (representative clusters circled in white); and a single (orange) cluster which spans the entire field of view.

We have proposed three approaches which, rather than shying away from disorder, use disorder to advantage in order to detect and characterize mesoscale and multi scale order in electronic systems (such as electron nematics) which break the rotational symmetry of the host crystal: (1) Extracting critical exponents from observed multi scale pattern formation in image data via cluster analyses.[7, 10]; (2) Manifestations of nonequilibrium behavior such as hysteresis[25, 26]; and (3) Noise characteristics[27, 28].

Method # 1 (Cluster Analyses) above is the subject of this paper, and the key insight is that near criticality, most physical quantities display power law behavior on length scales smaller than an appropriately defined correlation length. In order to make the connection with image data, this requires translating the geometric patterns into critical exponents, as described below.[7, 10] Method #2 (Hysteresis) relies on the extreme critical slowing down accompanying certain classes of quenched disorder.[29] For systems in which the quenched disorder is of the *random field* type (see Eqn. 1 below), hysteresis is a prominent and robust feature, which means that hysteresis can be a good diagnostic tool for order pa-

rameters which couple to material disorder via a random field mechanism.[28] In this case, we have proposed using hysteresis in order to detect disordered electron nematics, even ones which never fully order but exhibit only local nematic order. The key insight is to field cool in an orienting field (such as uniaxial pressure), and measure any macroscopic response function which is sensitive to nematic order (such as anisotropic resistivity). Through specific field cooling and orientational field switching protocols as described in Ref. [25], the presence of a disordered electron nematic can be revealed experimentally.[26] Method #3 (Noise Characteristics) above concerns another manifestation of the slow time dynamics associated with random field disorder. For example, very slow telegraph noise was observed in the transport properties of a YBCO nanowire in the pseudogap phase[27], consistent with the expected resistivity fluctuations of mesoscale electron nematic patches thermally switching their orientation.[28].

Patterns of unidirectional domains have been detected on the surface of cuprate superconductors.[11] In Fig. 1(a) and (b), we show the patterns of vertically oriented and horizontally oriented stripe domains, respectively, derived from a local Fourier transform of the R-map of STM on Dy-Bi2212, from Supplementary Fig. S3 of Ref. [11], as detailed in Ref. [10]. Fig. 1(c) shows the corresponding Ising cluster map, where orange represents vertically aligned clusters, and blue represents horizontally aligned clusters. From the figure, it is evident that there is one large system-spanning (orange) cluster. There are also several medium-sized clusters (some are circled in white in Fig. 1(c)), as well as many small clusters (circled in green in Fig. 1(c)).

The clusters display structure on all length scales within the field of view. In addition, as we will show below, the boundaries of the clusters are fractal, and the sizes of the clusters are power law distributed. These are all features which point to the pattern formation being driven by proximity to a critical point. If there is an underlying critical point driving the pattern formation, then critical exponents are encoded in the image.[7, 10]. For example, the number of clusters  $D$  of a particular size  $S$  is power-law distributed in this image,  $D(S) \propto S^{-\tau}$ , with a power set by the Fisher exponent  $\tau$ . In addition, the fractal geometric structure of the clusters can be quantified as the hull fractal dimension,  $d_h$ , and the volume (interior) fractal dimension,  $d_v$  of clusters. By studying the orientational analogue of the spin-spin correlation function, the anomalous dimension  $\eta_{||}$  can also be extracted from the image.

Relating these critical exponents to a particular fixed point requires a model. Near a critical point, the correlation length grows to become the dominant length scale, and it is possible to map the real physical system to a coarse-grained model with the same universal features. Starting from the cluster map in Fig. 1(c), we assign Ising

variable  $\sigma = 1$  to vertical domains, and  $\sigma = -1$  to horizontal domains.[10] We furthermore incorporate disorder into the model in the following way: In any given region of the sample, dopant disorder locally breaks the rotational symmetry of the Cu-O plane. (The same is true of other sources of quenched disorder.) This locally favors one orientation of the nematic over the other. Thus, quenched disorder acts as a random field on the local director of the Ising nematic.[28] The model may be stated as

$$H = - \sum_{\langle ij \rangle_{\parallel}} J_{\parallel} \sigma_i \sigma_j - \sum_{\langle ij \rangle_{\perp}} J_{\perp} \sigma_i \sigma_j - \sum_i h_i \sigma_i, \quad (1)$$

where the sum runs over the coarse-grained regions (Ising sites) consisting of a cubic lattice, chosen with spacing comparable to the resolution of the image(s) to be studied. The tendency for neighboring regions to be of like character is modeled as a nearest neighbor ferromagnetic interaction  $J > 0$ . The layered structure of the material is captured by the in-plane coupling  $J_{\parallel}$  being larger than the coupling between planes  $J_{\perp}$ . Ultimately, the criticality of such a quasi-two-dimensional system is controlled by a three dimensional fixed point for any finite  $J_{\perp}$ . However, in a strongly layered system such as the cuprates where  $J_{\perp} \ll J_{\parallel}$ , it is possible to observe a drift from two dimensional to three dimensional exponents when observing a finite field of view.[30]

There are six critical fixed points which can arise from the model of Eqn. 1: In the limit of zero disorder strength, the phase transition from disordered to long-range ordered nematic is controlled by the two-dimensional clean Ising model (C-2D) if  $J_{\perp} = 0$ , or by the three-dimensional clean Ising model (C-3D) for any nonzero coupling between planes. Random field disorder is relevant, and so the presence of any finite amount of random field disorder  $\Delta$  shifts the universality class to either the two-dimensional random field Ising model (RF-2D) or the three-dimensional random field Ising model (RF-3D).[10] Note that quenched material disorder can also give rise to randomness in the coupling strengths  $J_{\perp}$  and  $J_{\parallel}$ , also known as random bond disorder. However, in the presence of both random bond and random field disorder, the critical behavior is always controlled by the random field fixed point. For completeness, we also consider the possibility that the observed local orientations are not arising from an interacting model, which corresponds to the percolation fixed points which occur at the infinite temperature limit of Eqn. 1 as a function of applied orienting field. These are the two-dimensional and three-dimensional uncorrelated percolation points, P-2D and P-3D, respectively.

As shown in Fig. 1(c), there is one large spanning cluster, and there are several medium-sized clusters, and even more small clusters. By counting the number of clusters

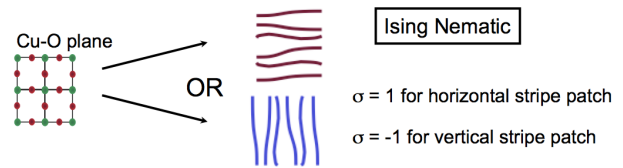


FIG. 2. An electron nematic breaks the rotational symmetry of the host crystal, in this case from C4 to C2 symmetry. The electron nematic then aligns either “vertically” or “horizontally.” We assign Ising variables  $\sigma = -1$  and  $\sigma = +1$ , respectively.

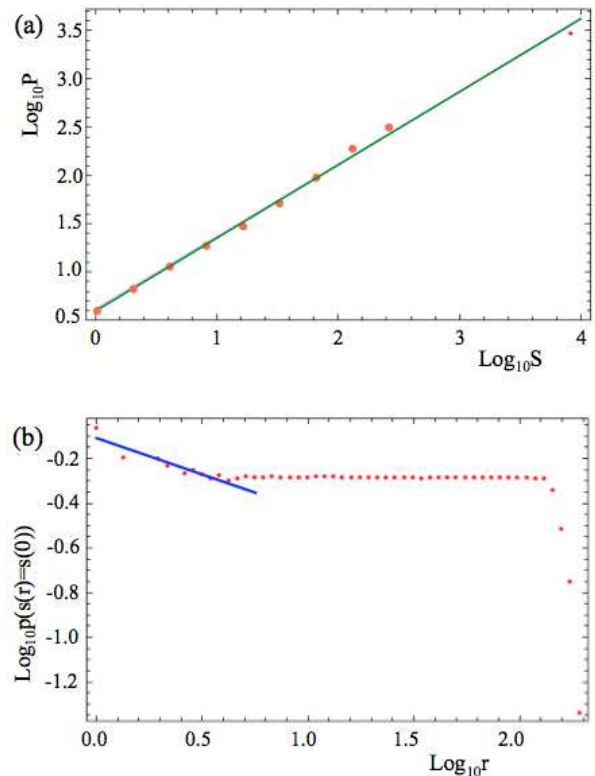


FIG. 3. Scale-free behavior of electron nematic clusters in Dy-Bi2212. (a) For each cluster size  $S$  (defined as the number of sites  $S$  in the cluster), the average perimeter is plotted. Scaling is evident throughout the entire field of view. Green line is a linear fit, yielding the ratio of fractal dimensions as described in the text. (b) The probability  $p$  that two spins a distance  $r$  apart are aligned. The blue line is a linear fit, as described in the text. In both panels, logarithmic binning has been used, which is a standard technique for power law analysis.[31]

$D$  of each size  $S$  (where  $S$  is the number of Ising sites in each cluster), one can construct the cluster size distribution  $D(S)$ . Near a critical point, this quantity exhibits power law scaling, as  $D(S) \propto S^{-\tau}$ . However, it is known that near criticality, the scaling function which forms the prefactor for the power law has a pronounced bump[32], at least for the 3D random field fixed point. Therefore, a

finite-size field of view is expected to underestimate the true value of  $\tau$ . In future experiments, larger fields of view can mitigate this effect. Within the field of view available, we find that a straightforward power law fit yields  $\tau = 1.71 \pm 0.07$ .

From the cluster structure in Fig. 1, one can see that the clusters themselves are not compact. Rather, they are ethereal, even gossamery[33] in nature. Indeed, both the boundaries and the interiors of the clusters are fractal in nature. In Fig. 3(a), we show a log-log plot of the average perimeter  $P$  of clusters of each size  $S$ . As with the cluster size distribution, a robust power law emerges throughout the entire field of view. By comparing the perimeter and cluster sizes, the ratio of fractal dimensions  $P \propto S^{d^*_h/d^*_v}$  can be extracted, where  $d_h$  and  $d_v$  denote the hull and volume fractal dimensions, respectively. (Here, the asterisk denotes the fact that only a 2D slice of the clusters is experimentally accessible, and there-

fore a corresponding geometric factor must be applied before comparing directly with 3D models.[10]) The ratio of fractal dimensions thus obtained is  $d^*_h/d^*_v = 0.78 \pm 0.01$ .

In Fig. 3(b), we plot the probability  $p(r)$  that two pseudospins  $\sigma = \pm 1$  a distance  $r$  apart are aligned. This is linearly related to the spin-spin correlation function  $g(r) \propto p(r)$ . (In the physical system, the spin-spin correlation function corresponds to the orientation-orientation correlation function of the director of the electron nematic.) The spin-spin correlation function becomes power law near a critical point,  $g(r) \propto 1/r^{d-2+\eta_{||}}$ . Here, we denote by  $\eta_{||}$  the anomalous dimension  $\eta$  at the surface of a material. As can be seen in the figure, this function is at most weakly power law in the data, with less than a decade of scaling. As such, this is the least reliable critical exponent extracted from the cluster analysis, yielding a value  $d - 2 + \eta_{||} = 0.8 \pm 0.3$ .

Exponent ↓; Model →	C-2D	C-3D	P-2D	P-3D	RF-2D	RF-3D	Dy-Bi2212
$\tau$	2.076	2.21	2.02	2.18	2.0	$2.02 \pm 0.03$	$1.71 \pm 0.07$
$d^*_h/d^*_v$	0.71	-	0.92	0.74	.92	0.57	$0.78 \pm 0.01$
$d - 2 + \eta_{  }$	0.25	2.54	0.207	0.93	1	0.336	$0.8 \pm 0.3$

TABLE I. Comparing critical exponents derived from R-Map STM data on Dy-Bi2212 to theoretical values of critical fixed points of the model in Eqn. 1. Critical fixed points considered include the clean two-dimensional and three-dimensional Ising models (C-2D and C-3D, respectively); uncorrelated percolation in two dimensions (P-2D); and the two-dimensional and three-dimensional random field Ising models (RF-2D and RF-3D, respectively). Theoretical values of fixed points are from Ref. [10] and references therein.

Table I shows a comparison between the critical exponents derived from the observed unidirectional electronic clusters in Dy-Bi2212 and theoretical values from critical fixed points of Eqn. 1. Note that for layered clean and random field Ising models, it is possible to observe a drift from 2D to 3D exponents in going from smaller to larger fields of view.[30] However, no such dimensional crossover makes sense when considering uncorrelated percolation.

We now compare the data-derived exponents against theoretical models. Note that the value of  $\tau$  from the data is lower than the theoretical value of every fixed point. This is expected for a finite field of view in random field models, where it is known that the cluster size distribution  $D(S)$  has a pronounced scaling bump.[32] Note also that there is not much variation in the theoretical values of  $\tau$  among the fixed points, so that while the presence of a robust power law in  $D(S)$  in the data is significant, it is difficult in principle to determine *which* fixed point could be responsible for the scale-free behav-

ior via this exponent.

By contrast, the anomalous exponent  $d - 2 + \eta_{||}$  shows a wide variation among fixed points, and can in principle be a good value to distinguish among fixed points. Unfortunately, the data-derived value has rather large error bars due to a limited regime of scaling, and so yields little information in this case.

Solid information can be gleaned by comparing the effective ratio of fractal dimensions,  $d^*_h/d^*_v$ . For 2D models, this corresponds to the bulk fractal dimensions,  $d^*_h/d^*_v = d_h/d_v$ . For 3D models, the bulk fractal dimensions differ from those observed on a 2D slice via geometrical factors, so that  $d^*_h/d^*_v = 3d_h/(4d_v)$ . [10] This ratio shows distinguishable variation among fixed points, and the data-derived value has small error bars and exhibits decades of scaling. All of this means that this exponent ratio is useful for distinguishing among the fixed points. Note that the observed ratio is inconsistent with uncorrelated 2D percolation (P-2D), and we can rule

out this fixed point as the origin of the pattern formation. Although the P-3D fixed point may appear to be a reasonable match, other considerations rule this out as the origin of the cluster pattern. First, this fixed point occurs when 31% of domains point one direction, and the rest point the other.[34] Such an extreme value of net nematicity would surely have been observed in macroscopic measurements on Dy-Bi2212, which is not the case. Second, while P-3D corresponds to the point at which geometric clusters percolate in a 3D system, this is not the same as the point at which those clusters percolate on a slice. Rather, at the 3D percolation point when *viewed on a 2D slice*, there is one large spanning cluster with many small clusters, and no robust power law behavior on the slice. So, the P-3D point can also be ruled out as the origin of the complex pattern formation.

This leaves the possibility of a dimensional crossover from 2D to 3D behavior in either the clean or random field Ising models. The expectation in the literature is that there should be no well-defined fractal dimension of geometric clusters at C-3D, since in fact geometric clusters do not exhibit power law behavior at the C-3D point.[35] However, recent studies indicate that when viewed *on a 2D slice*, geometric clusters do exhibit power law behavior at C-3D.[36] The ratio of fractal dimensions on a 2D slice is not known in this case, and will be discussed in a future publication.[37]

The possibility of a dimensional crossover from 2D to 3D exponents in a layered random field model is consistent with all data-derived exponents, and is the most likely source of the observed scale-free pattern formation of the electron nematic. In contrast with the clean model, geometric clusters do exhibit fractal dimensions and scale-free behavior at the RF-3D fixed point. Furthermore, if this identification is correct, then the clear prediction is that all data-derived exponents should drift away from the RF-2D values and closer to the RF-3D values upon increasing the field of view.

Other considerations also point to random field behavior: It has been previously shown that the slow telegraph noise observed in transport on a YBCO nanowire in the pseudogap regime[27] is consistent with the mapping of electron nematic domains in a host crystal to the random field Ising model.[28] This identification also serves to unify several experiments, in that it offers a concrete explanation for why certain materials display long-range orientational stripe order, and others do not. While true long-range electron nematic order is possible in a real 3D system, it is completely forbidden in a 2D system in the presence of any nonzero random field disorder. Thus, in a highly layered system such as the cuprates, many samples are expected to display no long-range order of the electron nematic, although in a layered RFIM, nematic clusters can grow quite large within the plane even if true long-range order is never achieved.[20, 30]

The RF-3D fixed point is a zero temperature fixed

point, which has implications for dynamics as well as future experimental tests of the critical exponents. First, it means that the entire finite-temperature phase transition boundary in the layered model exhibits extreme critical slowing down. With typical critical slowing down, the relaxation time of the system diverges as a power law as criticality is approached,  $\tau_{\text{relax}} \propto 1/|T - T_c|^{-\nu z}$ . However, the dynamics of the 3D random field Ising model are even more extreme near criticality, with the relaxation time diverging *exponentially* as criticality is approached,  $\tau_{\text{relax}} \propto \exp[\xi^\theta]$  where  $\xi$  is the spin-spin correlation length (which here corresponds to the orientation-orientation correlation length of the nematic director), and  $\theta$  is the violation of hyperscaling exponent, which is nonzero at this fixed point.[29] Second, because  $\theta \neq 0$  at a zero temperature fixed point, hyperscaling relations of critical exponents (which involve the dimension of the underlying phenomenon) must be modified.[29] Third, there is the question of whether fine-tuning is required to see power law behavior associated with the RF-3D fixed point. In fact, partly because it is a zero temperature fixed point with pronounced nonequilibrium effects, there is a wide critical region associated with this fixed point. For example, in the zero temperature 3D RFIM, critical behavior with 2 decades of scaling can be observed even 50% away from the critical point.[32]

Finally, we comment on the implications of multiscale behavior in cuprate superconductors. It is not just the electron nematic which exhibits fractal behavior in a bismuth-based cuprate, but similar behavior has been noted in the lanthanum family of cuprates as well. The local density of oxygen interstitials in LaSrCuO follows a power law at optimal doping.[7] In addition, theoretical studies have shown that there is a Goldilocks type of optimal inhomogeneity (neither too little nor too much) which favors superconductivity in a strongly correlated electronic system.[38, 39] The presence of inhomogeneity on multiple length scales, with robust power laws, in both the doping concentrations and also directly in the electronic degrees of freedom may point to the optimal inhomogeneity being fractal in nature. Much like the construction of the Eiffel tower incorporates elements of a scale-free iron latticework in order to optimize structural stability given a certain amount of iron to work with, high temperature superconductors may benefit from scale-free organization of electronic degrees of freedom in order to optimize the superconducting transition temperature.[40]

In summary, we conclude that the complex, scale-free pattern[10] of nematic clusters observed at the surface of Dy-Bi2212 via STM[11] is controlled by the 3D random field Ising model fixed point. That is, the ethereal cluster structure is due to a combination of interactions between clusters and quenched disorder due to material defects throughout the bulk of the material. As such, the pattern formation is not merely a surface effect. Rather, the nematic clusters form deep inside the material, and inter-

sect the surface. While this analysis cannot distinguish between true macroscopic long-range order of the electron nematic and short-range order, we can conclude that there is significant *multiscale* order in the system. Indeed, because the pairing energy scale is high, the pairing mechanism can arise from short-distance physics, and the presence of large nematic clusters throughout the bulk of the material is sufficient for superconducting pairing to originate from the electron nematic.

We thank J. Hoffman, S. Kivelson, Y. Loh, E. Main, B. Phillabaum, and C.-L. Song for helpful conversations. S.L. and E.W.C. acknowledge support from NSF Grant No. DMR 11-06187. K.A.D. acknowledges support from NSF Grant No. DMR 10-05209 and NSF Grant No. DMS 10-69224.

- 
- [1] E. Dagotto, *Science* **309**, 257 (2005).
- [2] K. Lai, M. Nakamura, W. Kundhikanjana, M. Kawasaki, Y. Tokura, M. Kelly, and Z. Shen, *Science* **329**, 190 (2010).
- [3] M. M. Qazilbash, M. Brehm, B.-G. Chae, P.-C. Ho, G. O. Andreev, B.-J. Kim, S. J. Yun, A. V. Balatsky, M. B. Maple, F. Keilmann, H.-T. Kim, and D. N. Basov, *Science* **318**, 1750 (2007).
- [4] Z. Sun, J. Douglas, A. Fedorov, Y. Chuang, H. Zheng, J. Mitchell, and D. Dessau, *Nature physics* **3**, 248 (2007).
- [5] J. M. Tranquada, B. J. Sternlieb, J. D. Axe, Y. Nakamura, and S. Uchida, *Nature* **375**, 561 (1995).
- [6] J. Zaanen and O. Gunnarsson, *Phys. Rev. B* **40**, 7391 (1989).
- [7] M. Fratini, N. Poccia, A. Ricci, G. Campi, M. Burghammer, G. Aeppli, and A. Bianconi, *Nature* **466**, 841 (2010).
- [8] R. W. Dull and H. R. Kerchner, “A teacher’s guide to superconductivity for high school students,” (1994), oRNL/M-3063/R1.
- [9] E. W. Carlson, V. J. Emery, S. A. Kivelson, and D. Orgad, “Concepts in high temperature superconductivity,” in *The Physics of Superconductors, Vol. II*, edited by J. Ketterson and K. Benneman (Springer-Verlag, 2004) in *The Physics of Superconductors, Vol. II*, ed. J. Ketterson and K. Benneman.
- [10] B. Phillabaum, E. W. Carlson, and K. A. Dahmen, *Nature Communications* **3**, 915 (2012).
- [11] Y. Kohsaka, C. Taylor, K. Fujita, A. Schmidt, C. Lupien, T. Hanaguri, M. Azuma, M. Takano, H. Eisaki, H. Takagi, S. Uchida, and J. C. Davis, *Science* **315**, 1380 (2007).
- [12] R. Borzi, *Science(Washington)* **315**, 214 (2007).
- [13] K. Cooper, M. Lilly, J. Eisenstein, L. Pfeiffer, and K. West, *Phys. Rev. B* **65**, 241313 (2002).
- [14] R. Du, D. Tsui, H. Stormer, L. Pfeiffer, K. Baldwin, and K. West, *Solid State Communications* **109**, 389 (1999).
- [15] E. Fradkin and S. Kivelson, *Science* **327**, 155 (2010).
- [16] Y. Ando, K. Segawa, S. Komiyama, and A. Lavrov, *Physical review letters* **88**, 137005 (2002).
- [17] V. Hinkov, S. Pailhes, P. Bourges, Y. Sidis, A. Ivanov, A. Kulakov, C. Lin, D. Chen, C. Bernhard, and B. Keimer, *Nature* **430**, 650 (2004).
- [18] R. Daou, J. Chang, D. Leboeuf, O. Cyr-Choiniere, F. Laliberte, N. Doiron-Leyraud, B. J. Ramshaw, R. Liang, D. A. Bonn, W. N. Hardy, and L. Taillefer, *Nature* **463**, 519 (2010).
- [19] C. Howald, H. Eisaki, N. Kaneko, and A. Kapitulnik, *Proceedings of the National Academy of Sciences of the United States of America* **100**, 9705 (2003).
- [20] M. J. Lawler, K. Fujita, J. Lee, A. R. Schmidt, Y. Kohsaka, C. K. Kim, H. Eisaki, S. Uchida, J. C. Davis, J. P. Sethna, and E.-A. Kim, *Nature* **466**, 347 (2010).
- [21] T.-M. Chuang, M. P. Allan, J. Lee, Y. Xie, N. Ni, S. L. Bud’ko, G. S. Boebinger, P. C. Canfield, and J. C. Davis, *Science* **327**, 181 (2010).
- [22] D. Abanin, S. Parameswaran, S. Kivelson, and S. Sondhi, *Phys. Rev. B* **82**, 035428 (2010).
- [23] O. Vafek and K. Yang, *Phys. Rev. B* **81**, 041401 (2010).
- [24] M. Rasolt, B. Halperin, and D. Vanderbilt, *Physical review letters* **57**, 126 (1986), predicts Valley Degeneracy Breaking in QHE.
- [25] E. W. Carlson and K. A. Dahmen, “Using disorder to detect locally ordered electron nematics via hysteresis,” Submitted to *Phys. Rev. Lett.*
- [26] C. Mirri, A. Dusza, S. Bastelberger, J. H. Chu, H. H. Kuo, I. R. Fisher, and L. Degiorgi, *Physical Review B* **89**, 060501 (2014).
- [27] J. Bonetti, D. Caplan, D. Van Harlingen, and M. Weissman, *Physical Review Letters* **93**, 087002 (2004).
- [28] E. W. Carlson, K. A. Dahmen, E. Fradkin, and S. A. Kivelson, *Physical Review Letters* **96**, 097003 (2006).
- [29] D. Fisher, *Physical Review Letters* **56**, 416 (1986).
- [30] O. Zachar and I. Zaliznyak, *Physical Review Letters* **91**, 036401 (2003).
- [31] M. E. J. Newman, *Contemporary Physics* **46**, 323 (2005).
- [32] O. Perković, K. Dahmen, and J. Sethna, *Physical Review Letters* **75**, 4528 (1995).
- [33] R. B. Laughlin, *Phys. Rev. Lett.* **79**, 1726 (1997).
- [34] D. Stauffer and A. Aharony, *Introduction to Percolation Theory* (Taylor & Francis, Philadelphia, 1991).
- [35] V. Dotsenko, M. Picco, P. Windey, G. Harris, E. Martinec, and E. Marinari, *Nuclear Physics B* **448**, 577 (1995).
- [36] A. A. Saberi and H. Dashti-Naserabadi, *EPL (Europhysics Letters)* **92**, 67005 (2011).
- [37] S. Liu, E. W. Carlson, and K. A. Dahmen, Forthcoming.
- [38] E. Arrigoni and S. Kivelson, *Physical Review B* **68**, 180503 (2003).
- [39] Y. Loh and E. Carlson, *Physical Review B* **75**, 132506 (2007).
- [40] N. Poccia, A. Ricci, and A. Bianconi, *Journal of Superconductivity and Novel Magnetism* **24**, 1195 (2011).